ISBN: 978-3-95450-214-1 ISSN: 2673-5490 doi:10.18429/JACoW-IPAC2021-WEPAB347

DESIGN, CONSTRUCTION AND TESTING OF A MAGNETIC PROBE FOR FAST KICKER MAGNETS

N. A. Cintas*, A. F. Colomo, T. Kramer, CERN, Geneva, Switzerland

Abstract

The CERN PS injection kicker has been modified in the framework of the LHC Injector Upgrade (LIU) project to allow injecting proton beams with an energy of 2 GeV. One of the most important items of the system parameter validation is the measurement and analysis of the magnetic field in the magnet aperture. To meet the required measurement precision without compromising the magnet vacuum performance, a dedicated magnetic probe has been designed, constructed and tested. The results are presented in this paper highlighting the mitigations of electrical, mechanical and vacuum complications. The paper concludes with an analysis of the probe performance during the first magnetic field measurements in the laboratory.

INTRODUCTION

In the framework of the LHC Injector Upgrade (LIU), the PS injection kicker (KFA45) needs to be upgraded to inject protons with energies up to 2 GeV [1,2]. To cope with the increased beam rigidity, several modifications in the kicker system have been deployed during recent years. The detailed modifications are outlined in [3-5]. To overcome this limitation a new KFA45 magnet has been designed and constructed [1]. To validate the new magnet performance, a fast magnetic probe has been designed, constructed and tested. This paper describes the electrical and mechanical design process and all material considerations to assure an acceptable measurement device compatible with ultra high vacuum (UHV) environments.

METHODOLOGY

Probe Design

A wire or stripline loop is commonly used as a tool to measure variable magnetic fields. To avoid complex designs, the stripline was made with a short circuit at the end. Furthermore, because of its short length, 337 mm, it can be considered as an ideal lossless transmission line. Therefore, measurements of its characteristic impedance and propagation time can be calculated in Eqs. (1) and (2), where L and C are respectively the inductance and capacitance per unit length (l).

$$Z_0 = \sqrt{\frac{L}{C}}, \quad (1)$$

$$\tau_D = \sqrt{LCl}. \quad (2)$$

To achieve a good signal integrity, impedance mismatches in the measurement set up need to be minimized. Keeping in mind that the majority of easily available coaxial cable impedance are either 50 Ω or 75 Ω, the stripline probe needs to approach these values. As shown in Eq. (1), its characteristic impedance depends on both, L and C, and those values depend exclusively on device materials and geometry. To accurately define a geometry that approaches the required impedance values, a transverse cut of the stripline probe was modeled in Opera©2D (see Fig. 1). After an iterative process, the probe geometry was finalized (Fig. 2) when a value of impedance was found close to the commercial value of 75 Ω but a little higher to take into account the isolation parts not included in the model which will reduce the final value of the impedance. Table 1 summarizes as built dimensions and its characteristic parameters.

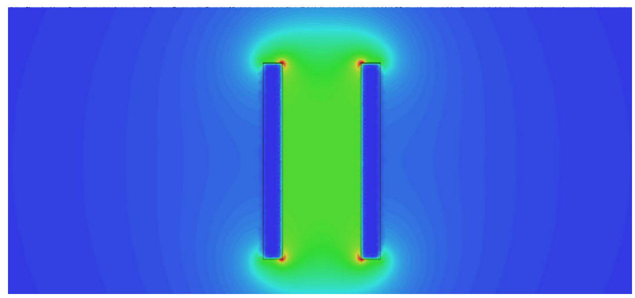

Figure 1: Magnetic field obtained when two parallel plates are simulated in Opera©2D.

Table 1: Final Probe Dimensions, Impedance and Propagation Time

Parameters	Value
Width	13 mm
Gap	4 mm
Inductance (L)	254 nH/m
Capacitance (C)	38 pF/m
Impedance (Z_0)	81 Ω
Propagation time (τ_D)	1 ns

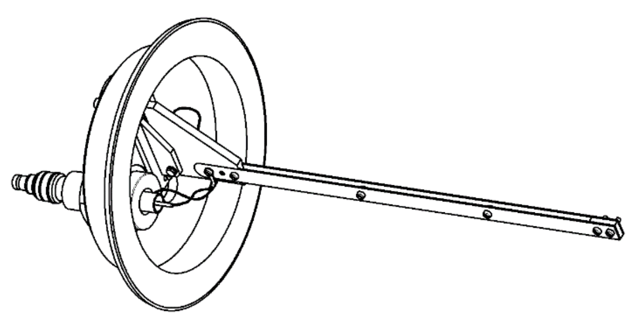

Figure 2: Drawing of the final probe design.

* nuria.ayala@cern.ch

ISBN: 978-3-95450-214-1 ISSN: 2673-5490 doi:10.18429/JACoW-IPAC2021-WEPAB347

As commented previously, all design considerations done in the model assumed a stripline geometry in vacuum. Although this is mostly true, the stripline needs to be isolated from the magnet flange by a ceramic support. In addition to that, several ceramic spacers have been used to keep the probe plates parallel. In our case, for vacuum compatibility reasons, Macor and ZrO_2 ceramics were chosen. These elements, placed in between the stripline plates, play a relevant role in the device capacitance due to their high dielectric constant (6 and 11 respectively). Analytic corrections to include the effects of ceramics suggested a final probe impedance of 62 Ω. Although this value is not exactly 50 or 75 Ω the deviation is small enough to still ensure a good signal integrity. To validate these corrections, measurements with the assembled probe including the ceramic spacers were done. A calibrated LCR meter was used to observe both, probe inductance and capacitance. The measurements were repeated at several frequency points and are summarized in Table 2. The values obtained are very similar to the theoretical ones, proving that all predictions were correct.

Table 2: Measured Characteristic Parameters of the Probe

Frequency	**L**	**C**	Z_0
10 kHz	100 nH	24 pF	65 Ω
100 kHz	90 nH	24 pF	61 Ω
1 MHz	90 nH	25 pF	61 Ω

Vacuum Considerations

The KFA45 operates inside a tank at High or even Ultra-High Vacuum (HV, UHV), that helps to reduce the aperture size. At the same time vacuum is a reliable dielectric (70 kV/cm^{-2} [6]) ensuring magnet operation under high voltage conditions. To minimize probe outgassing [7, 8], careful material selection was done. Outgassing rate of each material is listed in Table 3 [8].

Table 3: List of Materials Used in the Construction of the Probe [8]

Material	K_{10} **(mbar ls^{-1}cm^{-2})**
Aluminium (fresh)	$8.0x10^{-10}$
Copper (mech poliched)	$4.8x10^{-10}$
Stainless steel	$2.8x10^{-8}$
Brass	$1.3x10^{-8}$
Macor	–
ZrO_2	–
Polyamid (kapton)	$3.1x10^{-8}$
Viton A (fresh)	$1.5x10^{-8}$

A good electrical connection is needed between the stripline and the vacuum BNC feedthrough allowing the signal to be routed out of the vacuum tank. Among others, one of the biggest limitations when designing a device to be operated in a clean UHV environment is the replacement of soldering by another metal bonding technique. Standard SnPb soldering process contains volatile organic compounds not compatible at all with such demanding vacuum conditions. Two different solutions were developed: A commercially available vacuum compatible BNC contact to a coaxial kapton pigtail was used, this was then fitted with a lug and screwed to the probe copper (see Fig. 3 right). As a second option, an in house solution was developed. It consists of two multicontact pieces, for both inner and outer conductors. Pieces have been modified to be adapted to the feedthrough and also to get connected with a thick single-wire (Fig. 3 left). Finally, to minimize the inductance mismatch and keep a good signal integrity between the probe and the connector, a coaxial cable feedthrough was chosen. Due to the high water absorption and brightness of kapton [9], the pigtail length was minimized to degrade vacuum conditions as little as possible.

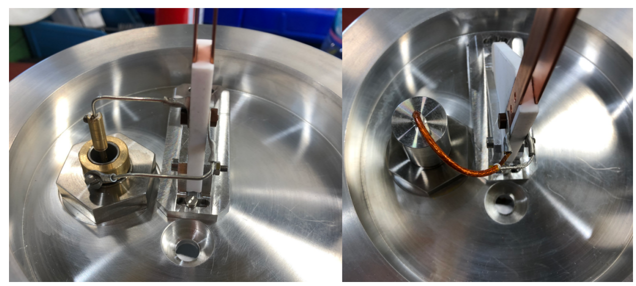

Figure 3: Two different options to connect the feedthrough to the probe loop. Left: using a homemade connection based on modified multicontacts. Right: Using an of the shelf connection solution.

RESULTS

In order to measure the magnetic field, the voltage induced in the probe needs to be integrated. There are different approaches to do so. The easiest is the digital integration tool of the scope, however any offset in the instrument will be integrated and will therefore distort the results. An alternative method based on an analogue RC filter integrator overcomes the offset problem. It integrates the measured signal and moreover attenuates the voltage amplitude at the oscilloscope input. For this last option, the only constraint to be defined is the time constant of the circuit. It has to be longer than the pulse length to avoid voltage drop due to the capacitor discharge. A time constant (τ) of hundred times the maximum pulse length was found as an optimal compromise between the mentioned factors. In case of the KFA45 kicker, the maximum pulse length is 2.45 µs, then τ = 245 µs. Figure 4 shows a comparison between the measured current pulse at the entrance of the magnet and the magnetic field measured by the probe. Since the probe is very short, its fine time resolution allowed to precisely observe fast magnetic field oscillations along the flat-top and post pulse. However, the probe could not be calibrated, meaning the shape of the pulse is obtained but not its real amplitude. Some equations

ISBN: 978-3-95450-214-1 ISSN: 2673-5490 doi:10.18429/JACoW-IPAC2021-WEPAB347

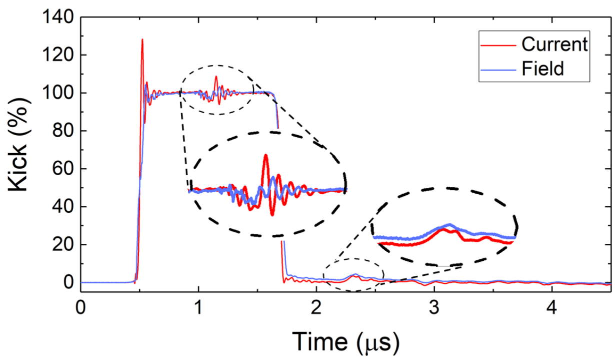

Figure 4: Normalized pulses comparison between current measured at the entrance of the magnet and the magnetic field measured with the probe plus the integrator.

were used to give an estimated value of the magnetic field amplitude. The formula used to do so is given by Eq. (3).

$$B_p = \frac{RCV_p}{d_{eq} l_m}. \quad (3)$$

RC is the time constant of the integrator, which was measured to be 236 µs. The equivalent distance between plates (d_{eq}) was estimated using Opera©2D and the value is 4.27 mm. l_m is the equivalent magnetic module length, 225.6 mm. To know if the obtained values are reasonable they were compared with the theoretical values of the field in the magnet aperture using Eq. (4), where I_m is the current measured at the entrance of the magnet module by a current transformer [10], and h_{ef} is the effective magnet aperture, in our case 54.06 mm.

$$B_t = \frac{\mu_0 I_m}{h_{ef}}. \quad (4)$$

Table 4: Magnetic Field Comparison between Theoretical Results (B_t) Et Measured by the Probe (B_p)

I_{meas} (kA)	B_t (mT)	B_p (mT)	$\Delta B/B_t$ (%)
0.88	20.5	18.6	13.7
1.32	30.7	28.2	13.2
1.74	40.5	37.2	13.2
2.15	49.9	46.1	12.5
2.57	59.7	55.1	12.8
2.80	65.2	58.1	13.9
2.98	69.2	63.2	13.7

Table 4 shows the theoretical and measured values of the magnetic field for different applied currents. There is a systematic error of around 14 % meaning those results are not valid for absolute measures but for comparative ones. For absolute measurements, a more complex design of the instrument should be considered in combination with a calibration procedure. It needs to be noted that the design aimed for a good time shape resolution of the magnetic probe and no additional consideration for absolute measurements were done.

This new tool has been used to improve the magnetic field pulse shape in order to be within the LIU specifications [1].

CONCLUSION

A magnetic probe has been designed and constructed to measure fast pulses in ultra high vacuum environment. Different considerations have been taken during the design: electromagnetic ones to adjust the characteristic impedance of the measurement set-up and material related ones, in order to avoid outgassing and vacuum leaks into the tank. This article gives the preliminary results of the measurements carried out with this new tool. Measurements with a good time resolution were achieved allowing to observe fast magnetic field changes. However, since the probe is not calibrated, the absolute magnetic values obtained through Eq. (3) can only be used to achieve comparative measurements which allows to analyse, improve and better understand the behavior of our pulse generator and magnet. A long probe has been constructed following the same procedure which measures multi magnets modules and studies any module to module coupling effect. Finally, a calibration is being considered in future designs for absolute field measurements.

ACKNOWLEDGEMENTS

The author would like to warmly thank N. Thaus and J.A. Ferreira (TE/VSC), L. Sermeus, R. Noulibos, L.M. Coralejo, Y. Sillanoli, S. Huon and P. Burkel (TE/ABT) for their important support. This work could not have been done without the help of all of them.

REFERENCES

[1] B. Goddard *et al.*, “Specification for Kicker Systems for 2 GeV PSB to PS Beam transfer”, in *Functional Specifications*, CERN, Geneva, Switzerland, 2015.

[2] T. Kramer *et al.*, “Considerations on the Fast Pulsed Magnet Systems for the 2 GeV Beam Transfer from the CERN PSB to PS”, in *Proc. 6th Int. Particle Accelerator Conf. (IPAC'15)*, Richmond, VA, USA, May 2015, pp. 3876–3878. doi:10.18429/JACoW-IPAC2015-THPF082

[3] T. Kramer *et al.*, “Analysis of the PS-Injection Kicker Performance, Improvements for and Impact on Operation LIU beams”, CERN, Geneva, Switzerland, Engineering Note, 2016.

[4] T. Kramer *et al.*, “Feasibility Study of the PS Injection for 2 GeV LIU Beams with an Upgraded KFA-45 Injection Kicker System Operating in Short Circuit Mode”, in *Proc. 7th Int. Particle Accelerator Conf. (IPAC'16)*, Busan, Korea, May 2016, pp. 1363–1366. doi:10.18429/JACoW-IPAC2016-TUPMR049

[5] T. Kramer *et al.*, “Performance of the PS Injection Kicker System Short Circuit Mode Upgrade for Operation with 2 GeV LIU Beams”, in *Proc. 8th Int. Particle Accelerator Conf. (IPAC'17)*, Copenhagen, Denmark, May 2017, pp. 3308–3311. doi:10.18429/JACoW-IPAC2017-WEPVA023

[6] M. J. Barnes *et al.*, “Injection and extraction magnets: kicker magnets”, CERN, Geneva, Switzerland, Rep. CERN-2010-004, Mar. 2011.

ISBN: 978-3-95450-214-1 ISSN: 2673-5490 doi:10.18429/JACoW-IPAC2021-WEPAB347

[7] M. Moraw, "Analysis of outgassing characteristics of metals", in *Vacuum*, vol. 36, pp. 523-525, Sep. 1986. doi:10.1016/0042-207X(86)90239-3

[8] L. de Chernatony, "Recent advances in elastomer technology for UHV applications", *Vacuum*, vol. 27, pp. 605-609, 1977. doi:10.1016/S0042-207X(77)80442-9

[9] R. J. Elsey, "Outgassing of vacuum materials-II", *Vacuum*, vol. 25, no. 8, pp. 347-361, Aug. 1975. doi:10.1016/0042-207X(75)91653-X

[10] Pearson Electronics Inc., "Pearson Current Monitor Model 110", 1999. http://pearsonelectronics.com/pdf/110.pdf